Fundamentals and Applications of Mo and Nb Alloying in High Performance Steels – Volume 1
Edited by Hardy Mohrbacher
CBMM, IMOA and TMS, 2014

AUSTENITE PROCESSING AND PHASE TRANSFORMATION OF NIOBIUM AND MOLYBDENUM ALLOYED HIGH PERFORMANCE STRUCTURAL STEEL

C.J. Shang[1], C.L. Miao[2] and S.V. Subramanian[3]

[1]University of Science and Technology Beijing, School of Materials Science and Engineering
Beijing, 100083, China
[2]Shougang Steel Group, Research Institute of Technology
Beijing, 100041, China
[3]McMaster University, Hamilton, Department of Materials Science and Engineering
Ontario L814L7, Canada

Keywords: High Performance Steel, Niobium, Molybdenum, Austenite Processing, Phase Transformation, Stress Relaxation, Thermal Simulation, CCT, Microstructure, Recrystallization, Austenite Grain Size, X80, X70, Dislocation Density, Microstructure

Abstract

Grain refinement and phase transformation control are significant issues for high performance structural steels. The use of a higher Nb content in low carbon Mn steel has an important effect on refining the prior austenite grains at intercritical temperatures by static recrystallization. The mechanism by which higher Nb levels produce ultra refinement of austenite is that recrystallization kinetics need longer incubation times and longer finish times, and higher solute Nb can slow down the mobility of recrystallized grain boundaries, and suppress grain coarsening effectively. Meanwhile, higher Nb can also suppress the softening between passes, and may increase the possibility of partial DRX (Dynamic Recrystallization) caused by high strain accumulation during hot strip finish rolling. Therefore, the start temperature of finish rolling should be lower to prevent DRX. Additionally, Nb and Mo are key elements for affecting phase transformation. Comparing results from an experimental Mn-Cr-Nb steel with Mn-Cr and Mn-Mo steels with higher Nb levels shows that a higher Nb content is beneficial in stabilizing austenite and widening the window for acicular ferrite and bainite formation during continuous accelerated cooling; whereas, Mo additions in low carbon higher Nb bearing steels widen the window for acicular ferrite and bainite transformation further. However, in order to obtain an optimum microstructure in low carbon-Mn-Nb-Mo steels, the ultra refined austenite should be cooled at a rate of more than 10 ºC/s, and the finish cooling temperature should be below 450 ºC.

Introduction

In order to meet the requirement of high performance, various metallurgical phenomena of Nb bearing low carbon low alloyed steels need to be controlled during the hot rolling and accelerated cooling process. No matter which rolling process is employed, grain refinement and strain accumulation of prior austenite grains are the key issues for obtaining excellent mechanical properties. In general, microstructure and properties are influenced by recovery of dislocations, static and dynamic recrystallization of austenite and precipitation. Literature [1] proves that increasing the Nb content in steel is the most effective method to retard SRX (Static

Recrystallization) compared with using other microalloying elements. Based on this characteristic, the higher Nb approach has been applied to rolled steel in a relatively higher non-recrystallization temperature range, the so-called high temperature process (HTP) [2]. Recent researchers [3,4] have shown that, in X80 pipeline steel, using a higher Nb content approach, the prior austenite grains can be refined from typically 80 microns to 10-20 microns and the elongated prior austenite grains can be flattened to several microns. Such a refinement effect is achieved by so-called "intercritical austenite processing" (IAP). According to the physical metallurgy principle of higher Nb bearing low carbon low alloyed steel, the rough rolling process should be optimized at an intercritical temperature to obtain an ultra fine and homogeneous prior austenite grain size by static recrystallization (SRX) with the solute dragging effect of dissolved Nb, while during the finish rolling process, the austenite should be flattened and strain accumulated in the non-recrystallization temperature range by not only precipitation but also the dragging effect of solute Nb.

Phase transformation after controlled rolling is another key factor affecting mechanical properties of steel, especially toughness. Generally, for low carbon low alloyed steel, Mo and Nb play important roles in phase transformation. Additionally, the accelerated cooling rate also significantly affects phase transformation. For the purpose of achieving high strength, high toughness and low cost, optimization of alloy design should be based on implementing an optimum TMCP process.

In this paper, the role of higher Nb contents on refining prior-austenite and accumulating strain in austenite will be introduced. Furthermore, the effect of Nb and Mo on phase transformation will be revealed. A skeleton map of an optimum TMCP process can be outlined for developing high strength, high toughness Nb bearing low carbon low alloyed structural steel.

Austenite Processing of Higher Nb Bearing Steel

Ultra Refining Prior Austenite Grains by Intercritical Static Recrystallization

Four low carbon steels were used for stress relaxation tests, as shown in Table I, therein, s1, s2 and s3 are laboratory steels with different Nb contents ranging from 0.012 wt% to 0.10 wt%, which were used to investigate the effect of niobium on recrystallization and precipitation behavior, and the possibility of grain refinement. Figure 1 presents the process cycle for the stress relaxation tests, after 25% reduction at a 1 s^{-1} strain rate at different temperatures, the specimens were held for 400 s at constant strain, and the stress-time curves were recorded. Actually, the stress relaxation method [5,6] can supply enough data to analyze the whole softening behavior as discrete events and can be used to characterize recovery or recrystallization behaviors, solute dragging and precipitation pinning. It is considered that more precise results can be obtained for isothermal recrystallization kinetics by the stress relaxation method [7].

Table I. Chemical Compositions of Experimental Steels Wt%

	C	Mn	Nb	Si	N(ppm)	Ni+Ti+Cu+Cr
s1	0.04	1.71	0.012	-	≤40	-
s2	0.04	1.76	0.063	-	≤40	-
s3	0.04	1.72	0.10	-	≤40	-
Industrial High Mn	0.04	1.75	0.095	0.22	≤40	<1.0 wt%

Figure 2 shows the stress relaxation curves of steels having different Nb contents, at 1050 °C and 1000 °C. According to Figure 2(a), no precipitation hardening was found at 1050 °C, and recrystallization softening occurs in all three steels after deformation, but the onset times of recrystallization are different; 0.10%Nb steel has the longest incubation period, less than 2 s, but the time for the 0.012%Nb steel is shorter than 0.5 s. Moreover, the 0.10%Nb steel needs a longer time to complete the recrystallization process compared with the other two steels. From the morphology of the austenite grains in Figure 3, partial recrystallization occurs in the 0.10%Nb steel at 2 s. Additionally, it is evident that most grains in the 0.10%Nb steel have finished complete recrystallization at 30 s, which is in agreement with the results of the stress relaxation test at 1050 °C.

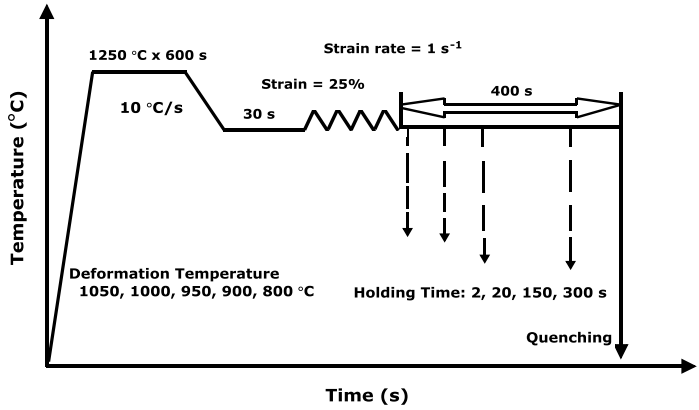

Figure 1. Schematic diagram of stress relaxation tests.

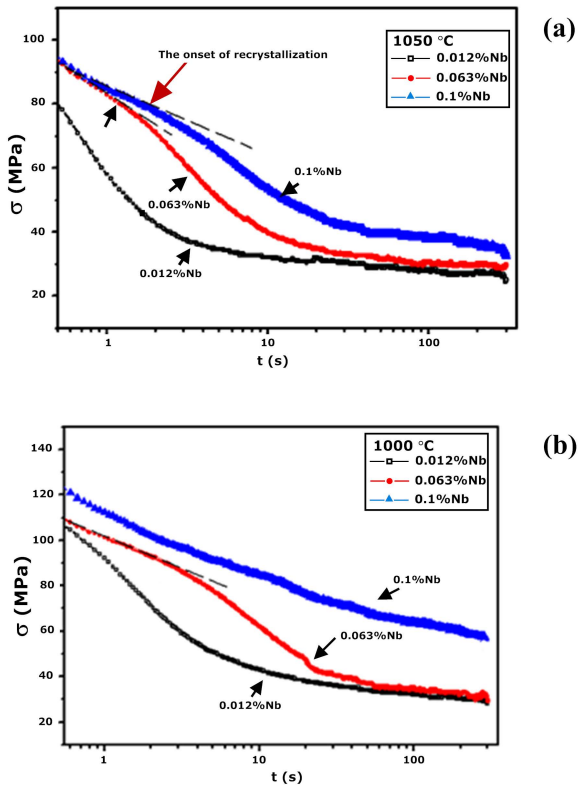

Figure 2. Stress relaxation curves; (a) 1050 °C, (b) 1000 °C.

Likewise, Figure 2(b) presents obvious recrystallization softening for the 0.063%Nb steel and 0.012%Nb steels at 1000 ºC. Incubation time of recrystallization increased as the temperature decreased. It is interesting to see from the curve of the 0.10%Nb steel at 1000 ºC that no obvious accelerated softening by recrystallization as well as no suppressed softening by precipitation occurs. Actually, TEM observations on the specimen from the 0.10%Nb steel after 300 s holding did not reveal strain-induced precipitated particles [4]. Combined with the etching results of austenite grains shown in Figure 4, there is a very slow recrystallization process, which is also time dependent, just as in the case at 1050 ºC.

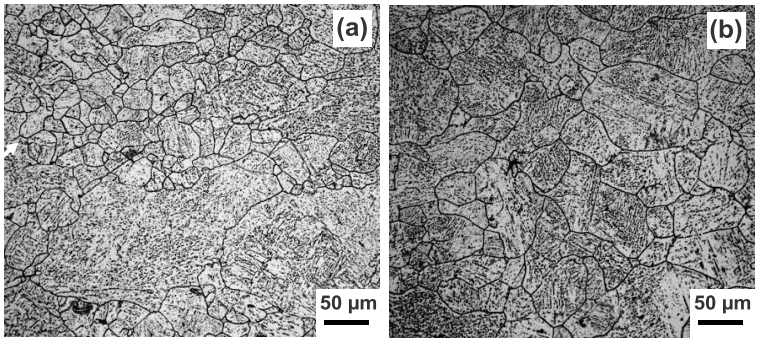

Figure 3. Morphology of austenite grains at 1050 °C; (a) 0.1%Nb - 2 s, (b) 0.1%Nb - 30 s.

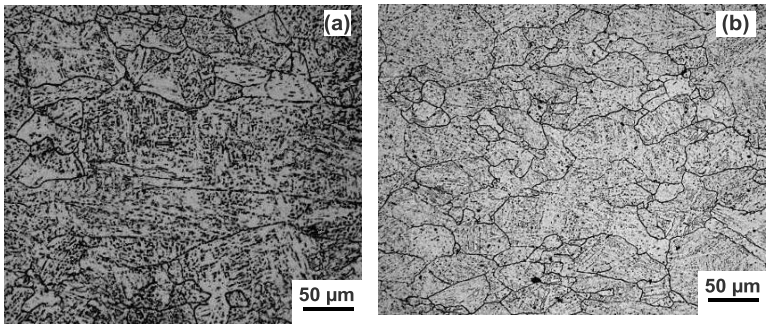

Figure 4. Morphology of austenite grains at 1000 °C; (a) 0.1%Nb - 30 s, (b) 0.1%Nb - 300 s.

Stress relaxation curves can effectively reflect recrystallization softening and precipitation hardening behavior [8]. From Figure 5, the curves from the 0.10%Nb steel at 950 ºC and 900 ºC both show the softening rates being reduced by strain-induced precipitation at 5 s and 3 s, respectively. It is also shown by TEM observation that precipitates are not found in the specimens of the 0.10%Nb steel at 2 s from 950 °C to 850 °C, however, after holding for 20 s, particles with a size ≤50 nm were observed, as shown in Figure 6.

The recrystallization behavior of a commercial higher Nb X80 pipeline steel was also examined. Its chemical composition is shown in Table I. The stress relaxation method was also employed for further research on recovery, recrystallization and precipitation, and a schematic of the process is shown in Figure 7.

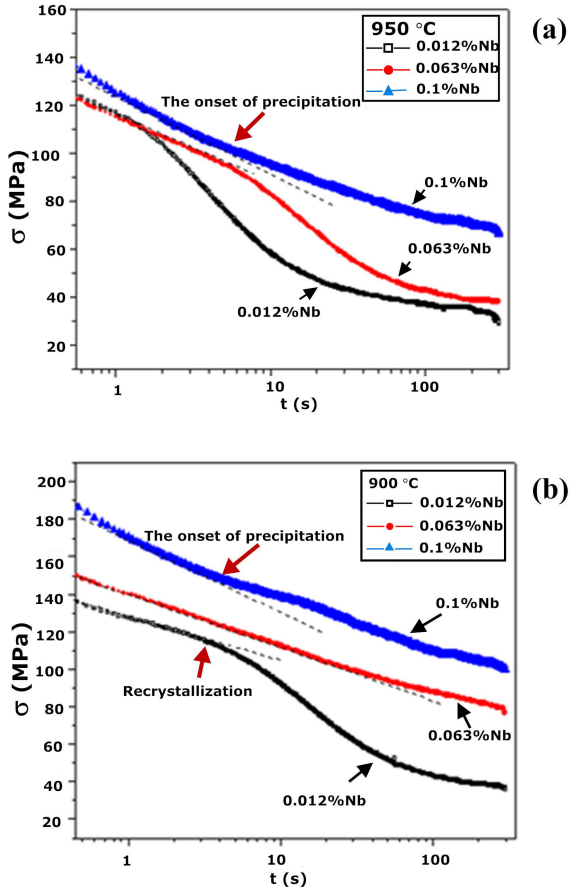

Figure 5. Stress relaxation curves at different temperatures; (a) 950 °C, (b) 900 °C.

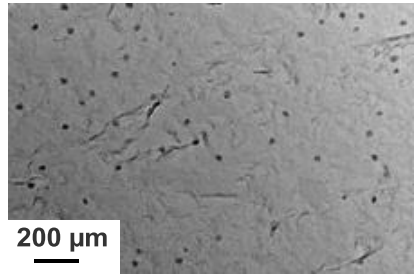

Figure 6. Morphology of strain induced precipitates at 950 °C in 0.1%Nb steel after delay of 20 s.

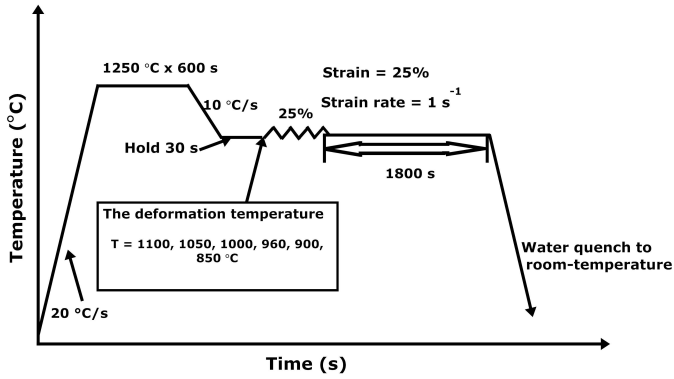

Figure 7. Thermomechanical process of stress relaxation tests for industrial steel.

Stress-relaxation curves for the industrial steel were measured at different temperatures. As shown in Figures 8(a) and (b), the stress level in the initial period falls quickly at 1100 ºC and 1050 ºC, due to the occurrence of recovery and recrystallization. When static recrystallization occurs, the relaxation time hardly reached 1 s, and the recrystallization stop time also is similar to the results from double compression tests. Once the relaxation temperature was decreased to 1000 ºC, as shown in Figure 8(c), visible softening behavior caused by recrystallization does not appear within 100 s. Neither is a hardening platform, resulting from strain-induced precipitation, clearly observed in this curve, that is to say, there are no precipitated particles available that can have their effect on dislocation mobility. Figure 8(d) indicates that strain-induced precipitation occurs after 25% prior deformation at 900 °C, and hardening behavior occurred after relaxing for 4 s.

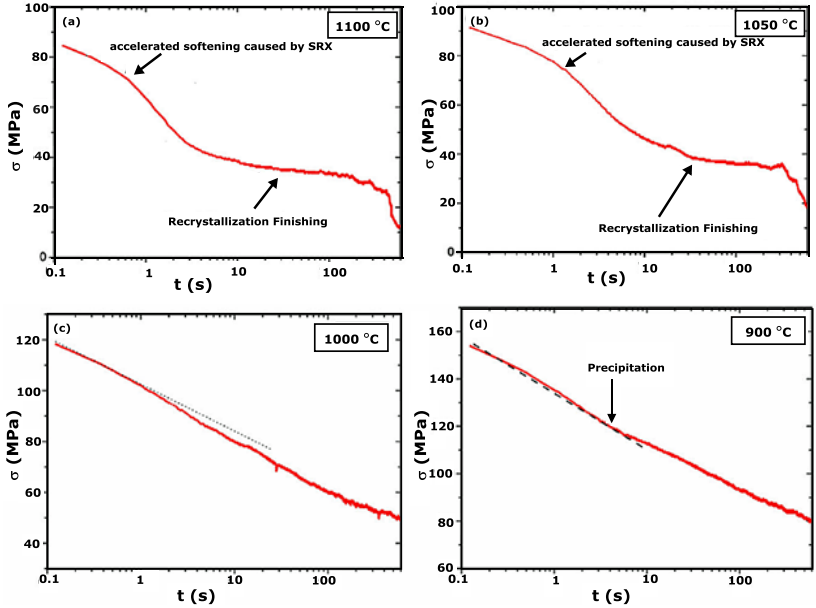

Figure 8. Stress-relaxation curves of Nb-bearing industrial steel at different temperatures; (a) 1100 °C, (b) 1050 °C, (c) 1000 °C, (d) 900 °C.

Likewise, similar thermo-simulation tests were also carried out on the industrial steel, as shown in Figure 9, and a statistical analysis of grain size distribution from the samples was analyzed by the software *image Pro* based on grain data in five different regions of each tested sample.

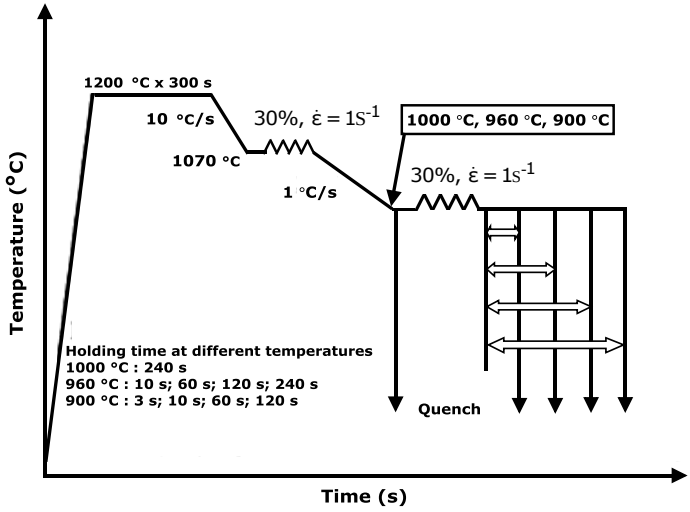

Figure 9. Thermomechanical schedule for observing morphology of prior austenite grains.

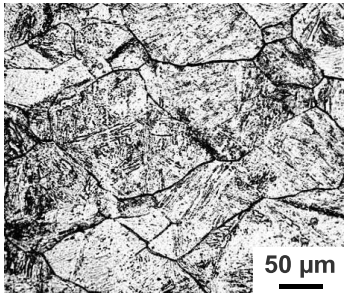

Figure 10. Morphology of the prior austenite grains.
(30% deformation at 1070 °C).

Figure 10 shows the morphology of statically recrystallized grains after 30% deformation at 1070 °C, it can be seen that the average size of completely recrystallized austenite grains is more than 80 µm. The accelerated recrystallization after the execution of one pass at 1070 °C is still time-dependent, as is the recrystallization of this steel after single deformation at 1050 °C. The recrystallization finishes in a very short time (less than 20 s). The morphology of the prior austenite grains after deformation and holding for 10 s, 60 s and 240 s is illustrated in Figure 11. Austenite grains after holding the sample for 10 s, Figure 11 (a), are homogenous and very fine, the average grain size is only about 19 µm, i.e. most austenite grains have finished SRX. Even

when holding for 240 s at 1000 °C, the average grain size is still less than 28 microns. The growth rate of recrystallized grains is relatively much slower compared with that at 1070 °C and this can be explained by the slow coarsening rate of recrystallized grains which results from the intense dragging effect of solute Nb.

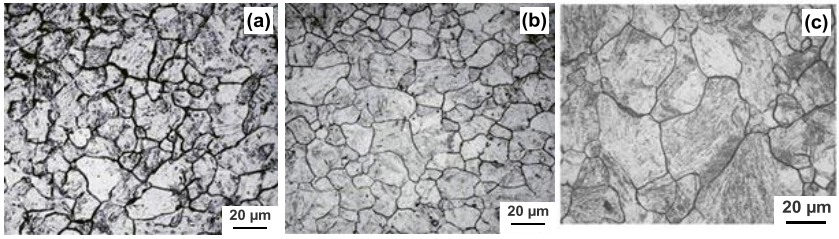

Figure 11. Stress relaxation curves of industrial steel under different conditions, and morphology of austenite grains at different times; (a) 10 s, (b) 60 s, (c) 240 s.

Preventing Dynamic Recrystallization by Optimizing Finish Rolling Process

In the present study, steels of two types (S and I) were analyzed, as shown in Table II. Steels of the first type (S2 and S3) were cast in the laboratory to solely investigate the effect of Nb on flow stress and DRX. The influence of other micro-alloyed elements can be eliminated. The steels of the second type (I2 and I4) were industrial X80 pipeline steels, with the aim to understand strain accumulation behavior during multi-pass rolling at relatively high temperatures. Cylindrical specimens of $\Phi 8 \times 10$ mm were prepared for the research on DRX before testing in a Gleeble-3800 thermo-mechanical simulator. The simulation schedule is shown in Figure 12. Specimens were reheated to 1100 °C for 120 s and then cooled to the test temperature (900-1100 °C) at 10 °C/s. After holding for 30 s at this temperature, the samples were compressed with 60% deformation at constant strain rates of 0.05-2 s^{-1}, and then quenched immediately.

Table II. Chemical Compositions of Investigated Steels

ID	C	Mn	Nb	Si	Mo	Cu+Ti+Ni+Cr
s2	0.037	1.76	0.063	-	-	
s3	0.031	1.72	0.10	-	-	
I2	0.044	1.83	0.092	0.18	0.249	0.54
I4	0.048	1.81	0.067	0.20	0.284	0.49

Figure 12 illustrates the simulated process of multi-pass rolling. Therein, the reductions and pass intervals are based on actual hot strip rolling of X80 pipeline steel. Strain-stress data were recorded for all simulated tests, and mean flow stress (MFS) values were calculated [9] in the analysis of this process.

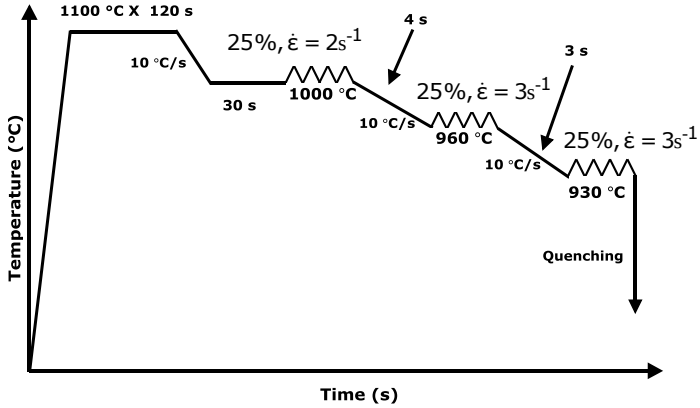

Figure 12. Schematic of simulated process for multi-pass deformation.

Figure 13 illustrates the stress-true strain curves and the evolution of mean flow stress in multi-pass rolling. There is a stress peak in the second pass for the industrial higher Nb steel and, also, its MFS value is decreased in the second pass. The decrease of the MFS value implies occurrence of DRX/MDRX during rolling, however the MFS value of the medium Nb steel increases steadily during rolling. The softening caused by DRX is only found in the higher Nb steel and hence the final stress values of these two steels are similar. Actually, the higher Nb steel has a larger critical strain value, so the occurrence of DRX can be explained by higher strain accumulation associated with the high Nb content. Moreover, the occurrence of DRX will generate serious mixed grain microstructures which have a negative impact on the toughness of the steel [10].

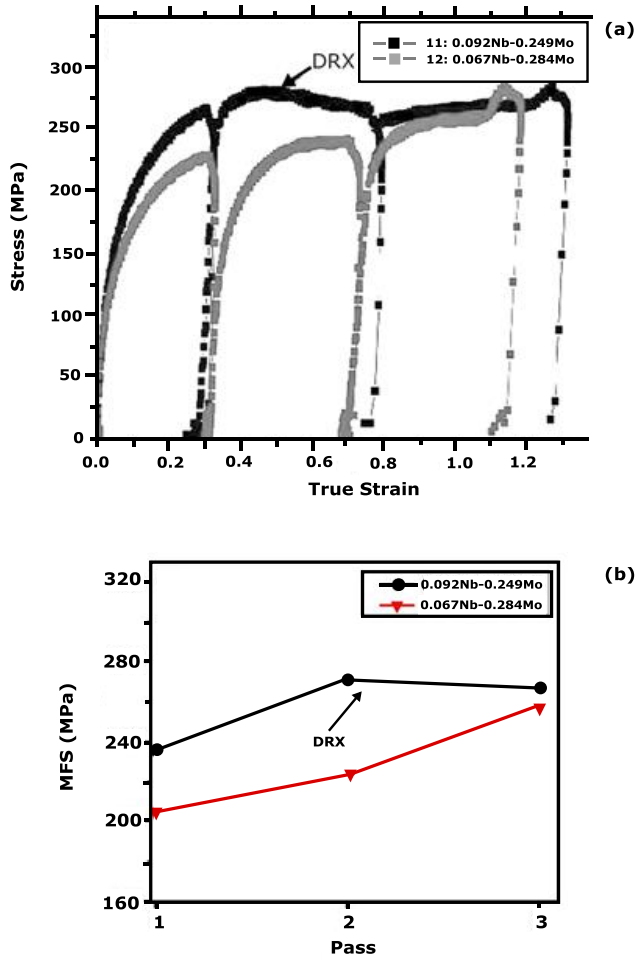

Figure 13. (a) True stress-strain curves and (b) mean flow stress (MFS) of multi-pass rolling.

A plane strain thermomechanical-simulation machine was used to investigate strain accumulation in the industrial steel, Table I; the schedule based on industrial rolling of X80 strip is shown in Figure 14 and was designed to focus on the effect of rolling temperature. Two finish rolling start temperatures were chosen, 940 °C and 910 °C, respectively, and true stress-strain curves were obtained.

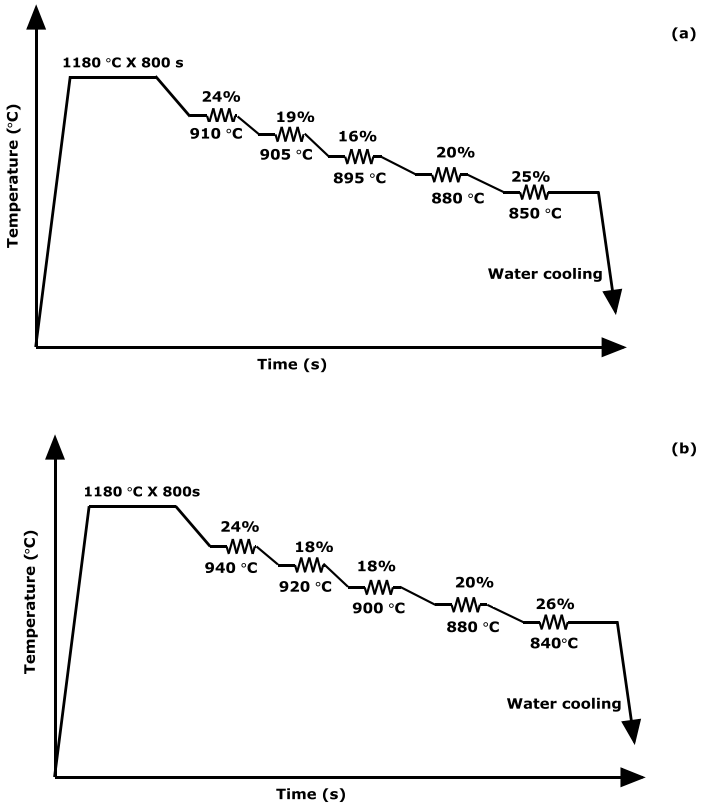

Figure 14. Schedule of plane strain tests.

In the high Mn higher Nb steel, the kinetics of strain-induced precipitation Nb(C,N) is offset by the higher Mn content [11]. The speed of finish rolling is very fast in industrial tandem rolling (the interstand time is very short), so there is hardly any available Nb(C,N) precipitated between passes. However, the dragging effect is still very strong. In this case, the strain accumulation by

rolling passes will easily reach a high level. Once the accumulated-strain exceeds a critical strain, dynamic recrystallization will take place [12].

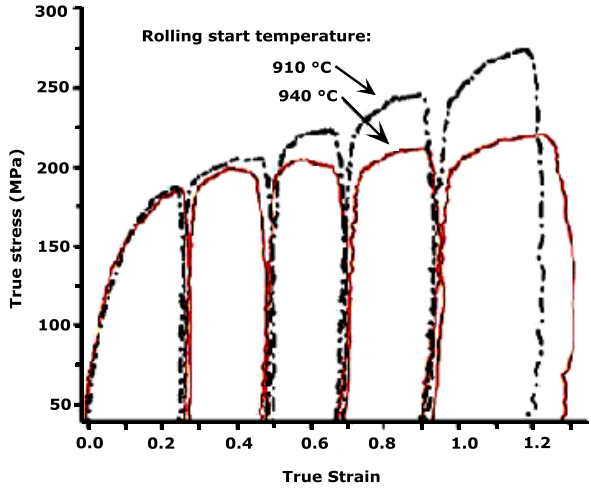

Figure 15. True stress-strain curves at different steps of plane strain simulation.

Figure 15 shows stress-strain curves measured in the plane strain test. In the first case where finish rolling starts at 910 °C, the stress value increases steadily. Yet, when the start/finish rolling temperature is raised to 940 °C, the characteristics of the stress-strain curve in the third pass indicate the occurrence of dynamic recrystallization. The same conclusion can be obtained when analyzing the mean flow stress (MFS). A drop of the MFS indicates the occurrence of DRX [13], as shown in Figure 16. In dynamic recrystallization, the relationship between the critical strain value and deformation temperature is inverse [14] which means that the critical strain value decreases with increasing temperature. If the rolling process (rolling reduction, strain rate, etc.) is not well defined, dynamic recrystallization is more likely to take place in a high temperature deformation process.

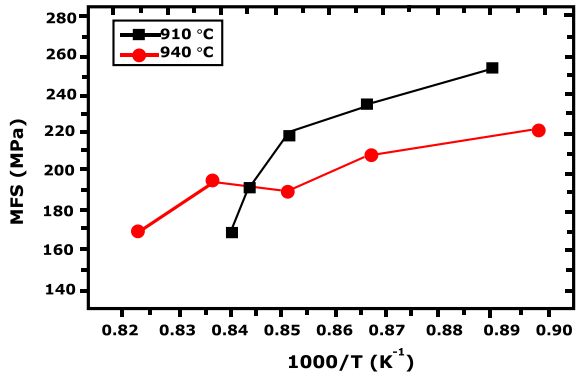

Figure 16. Mean flow stress (MFS) at different steps of plane strain simulation.

Prior austenite grains as shown in Figure 17(a) are homogeneous, for a rolling start temperature of 910 °C. However, austenite grains are non-uniform in Figure 17(b) for a start/finish rolling temperature of 940 °C and there is a grain layer, which is composed of small size grains among some coarse grains. Their morphology is like a necklace, which is probably caused by the occurrence of partial dynamic recrystallization. Generally, complete dynamic recrystallization evidently refines grain size, but partial dynamic recrystallization leads to serious mixed grain microstructures and a loss of dislocation density which would not be of benefit to strain accumulation in the austenite, resulting in a drop of yield strength.

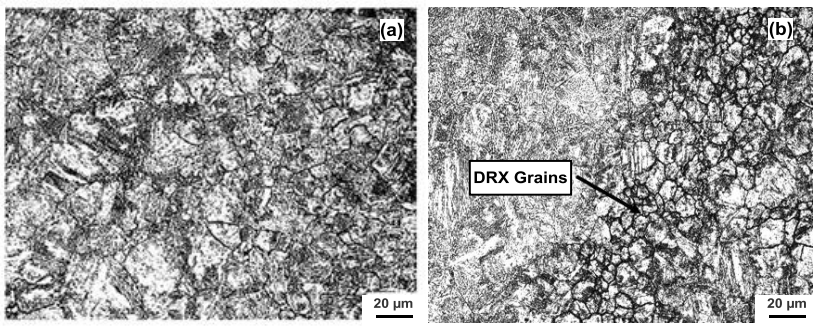

Figure 17. Morphology of prior austenite grains (vertical direction of rolling) for a start rolling temperature of (a) 910 °C, (b) 940 °C.

Combining these above characteristics of high Mn high Nb steel, a skeleton map can be outlined for optimization of the rolling schedule. Deforming above 1050 °C allows break up of coarse austenite grains, but due to the absence of precipitates and solute dragging effect in this temperature regime, grain growth and coarsening behavior is fast. Controlling rough rolling to further refine austenite grains, complete recrystallization will happen after deforming in the temperature range close to 1000 °C. The dragging effect from solute Nb can effectively retard the growth and coarsening of grains so that a homogeneous and fine grain structure can be obtained before finish rolling. Partial recrystallization must be avoided during finish rolling. By decreasing the rolling temperature and controlling reduction in each pass, pancaked austenite grains with a small width, will be obtained. Whether in plate or in strip rolling, high S_v (grain boundary area per unit volume) is always a key aim to acquire good properties for the steel. The flow stress level reflects the dislocation density. Actually, the flow stress behavior, both during and after deformation, is a key factor in determining the final dislocation density. The influence of the Nb content on flow stress behavior during deformation varies depending on temperatures and strain rates. In actual production, plate rolling has the metallurgical characteristics of a low strain rate and large deformation. Thus, higher Nb steels can provide a large advantage in effectively suppressing DRX behavior at high temperatures. A higher stress level or S_v is therefore easier to obtain at low temperature. However, in hot strip rolling a larger strain rate will be applied. Thus the influence of the Nb content on flow stress behavior will diminish during the finish rolling process. The main influencing factors for the final stress level are the softening and hardening behavior after deformation, which have a close correlation with the solute Nb content and precipitation. A high amount of solute Nb can prevent significant recovery between passes. Thus a higher Nb content can suppress softening between pass intervals, and may result in higher strain accumulation [15]. Although DRX of higher Nb steel requires a higher critical stress value, strain accumulation can still exceed it. Therefore the onset of DRX for higher Nb steel is more easily achieved during hot strip rolling (finish rolling process) with relatively high start rolling temperatures. However, by decreasing the finish rolling temperature, the DRX of high Mn higher Nb steel can be restrained, and a higher and steady MFS can be achieved. As a consequence, a homogeneous grain structure and a high S_v will be obtained.

Phase Transformation Characterization and Optimum Control of Process

Low carbon, high Mn, high Nb, Cr (Mo) alloy design has been accepted for the development of high strength pipeline and other infrastructural steels. Generally, Cr and Mo are added for solid solution strengthening. Solutes Cr, Mo and Nb also have an effect of increasing the hardenability. Actually, 0.04-0.08%C, 1.8-2.0%Mn and 0.08-0.1%Nb steel can transform to acicular ferrite and/or bainite by TMCP [16]. Cr, Mo, Ni and Cu can be added for further strengthening and/or increased hardenability. As the costs of Mo and Ni are relatively high, the added amount of alloying element should be justified by the strength grade required and also by the actual TMCP facility available. Nevertheless, the phase transformation characteristics of each alloying element should be understood, and the key processing parameters to produce the optimum microstructure in each kind of alloyed steel should be revealed.

The compositions of three experimental steels used in the research are shown in Table III. The Mn-Mo-Nb steel is the composition of conventional X70, and the Mn-Cr-Nb^+ and Mn-Mo-Nb^+ steel are higher Nb bearing grades used for X80 pipeline steel.

Table III. Chemical Composition of Three Experimental Steels in wt%

Experimental Steel	C	Si	Mn	Nb	Mo	Cr	Other microalloy elements
Mn-Mo-Nb	0.050	0.23	1.52	0.052	0.18	-	Ni+Al+Cu+Ti+V =0.09
Mn-Cr-Nb$^+$	0.043	0.16	1.90	0.091	-	0.29	Ni+Ti+Cu=0.42
Mn-Mo-Nb$^+$	0.026	0.14	1.92	0.090	0.15	-	Ni+Ti+Cu=0.42

Effect of Higher Nb and Mo on Continuous Cooling Phase Transformation

Static CCT diagrams for the steels were obtained by the thermal simulator FORMASTER. The specimens (3 mm diameter ×10 mm) were heated to 1000 ºC at 20 ºC/s, soaked for 500 s, and cooled to 900 ºC. After holding for 10 s at 900 ºC, the specimens were cooled to room temperature at rates of 0.5, 1, 3, 5, 10, 15, 20 ºC/s, respectively.

The CCT diagrams of the Mn-Mo-Nb and Mn-Cr-Nb$^+$ steels are shown in Figure 18(a). It can be seen that at lower cooling rates, the Mn-Mo-Nb steel is more likely to transform into ferrite-pearlite. When the cooling rate is higher than 5 ºC/s, the CCT curves of the two steels tend to be similar. When the cooling rate is larger than 10 ºC/s, both steels transform in the acicular ferrite and bainite zone. It is noticeable that the final phase transformation temperature of the Mn-Cr-Nb$^+$ steel is lower than that of the Mn-Mo-Nb steel. It can be concluded from a comparison of the results that the austenite of the higher Nb bearing steel is more stable, even without a Mo addition. Therefore, Mn-Mo-Nb steel can be replaced by Mn-Cr-Nb$^+$ steel, because identical phase transformation can be obtained when using a cooling rate of more than 10-15 ºC/s under accelerated cooling conditions. The key point of replacing Mn-Mo-Nb steel by Mn-Cr-Nb$^+$ steel is that the type and proportion of Mn-Cr-Nb$^+$ intermediate temperature transformation product can be controlled by cooling rate and final cooling temperature control within a certain range, however, cooling rate and cooling stop temperature are usually constrained by the mill facility. Furthermore, there is some difference between the physical metallurgy of a continuous hot rolling mill and a steckel-mill. All the factors stated above can influence the strength and toughness of pipeline steels. Considering the limitations of the facility, addition of Mo is taken account of in the higher Nb bearing alloy design.

Static CCT curves of the Mn-Mo-Nb$^+$ and Mn-Cr-Nb$^+$ steels are compared in Figure 18(b). The starting transformation temperature of the Mn-Cr-Nb$^+$ steel is higher than that of Mn-Mo-Nb$^+$ steel, and the ferrite and bainite zones of the Mn-Cr-Nb$^+$ steel are larger than those of the Mn-Mo-Nb$^+$ steel. That is because the addition of Mo retards the transformation to ferrite and pearlite, shifting the whole ferrite zone to longer times. It can also be concluded from Figure 18(b) that at higher cooling rates, the bainite transformation zone of the Mn-Cr-Nb$^+$ steel is wider. That is to say, with a higher starting transformation temperature it is feasible to obtain acicular ferrite and bainite. However, at lower cooling rates, bainite formation is more likely in Mn-Mo-Nb$^+$ steel.

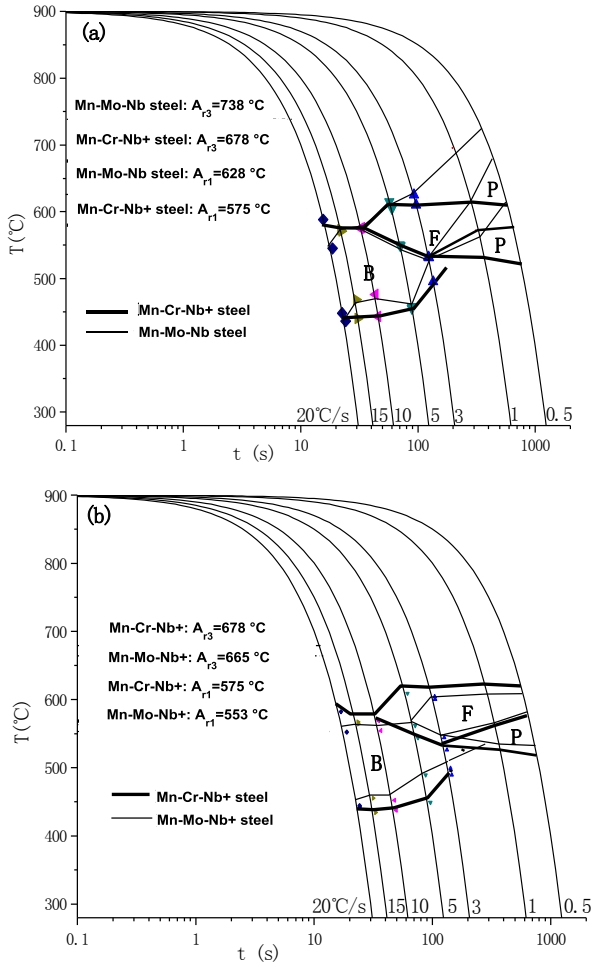

Figure 18. CCT diagram of experimental steels; (a) Mn-Mo-Nb and Mn-Cr-Nb+ steels, (b) Mn-Mo-Nb+ and Mn-Cr-Nb+ steels.
(Ar temperatures determined by continuous cooling from 900 ºC at 0.05 ºC/s).

Continuously cooled microstructures of the Mn-Cr-Nb^{+} steel at different cooling rates are shown in Figure 19. It can be seen that in Figure 19(a) and (b), at a cooling rate of 1 ºC/s, the microstructure is mostly composed of polygonal ferrite and quasi-polygonal ferrite, a small quantity of degenerate pearlite can also be observed. At a cooling rate of 5 ºC/s, the microstructure, Figure 19(c), is mostly composed of fine acicular ferrite, and a little polygonal ferrite. The microstructure at 10 ºC/s, Figure 19(d), is mostly evenly distributed acicular ferrite and when the cooling rate reaches 15 ºC/s, the microstructure, Figure 19(e) and (f), evolves to acicular ferrite and bainite, which are much finer than obtained at lower cooling rates.

Figure 20 shows that at a cooling rate of 3 ºC/s, more and finer bainite microstructures are formed. Mo can prohibit the phase transformation of austenite to ferrite, and increase the nucleation sites and thus a finer microstructure can be obtained in the presence of Mo. Moreover, the addition of Mo can promote the generation of bainite at relatively low cooling rates. Therefore, in industrial rolling, adding some Mo is a good choice to meet the requirement of strength.

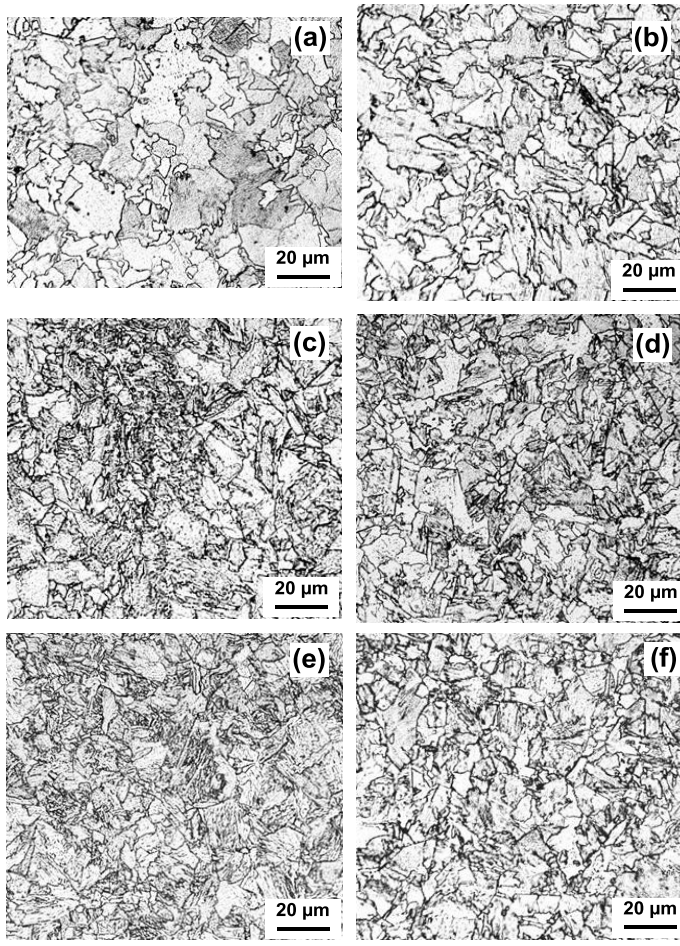

Figure 19. Continuous cooling microstructure of Mn-Cr-Nb+ steel; (a) 0.5 °C/s, (b) 1 °C/s, (c) 5 °C/s, (d) 10 °C/s, (e) 15 °C/s, (f) 20 °C/s.

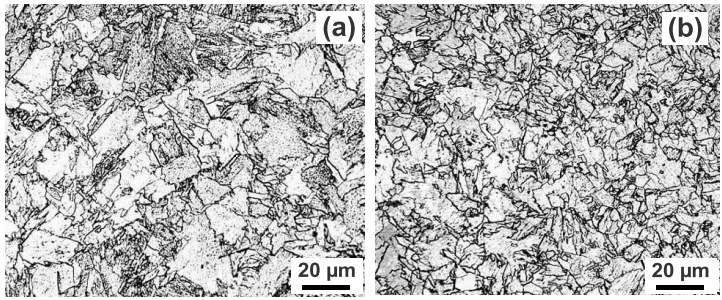

Figure 20. Microstructure of steels continuously cooled at 3 °C/s;
(a) Mn-Cr-Nb+, (b) Mn-Mo-Nb+.

Intermediate Phase Transformation Characteristics, Control of Cooling Start and Stop Temperature

Isothermal phase transformation research was also performed with the FORMASTER. The samples were heated to 1100 ºC at 20 ºC/s, held for 300 s, and then cooled to 650, 600, 550, 500 ºC at 60 ºC/s, respectively. After holding for 900 s at the above temperatures, the specimens were quenched to room temperature.

The microstructure of the Mn-Cr-Nb+ steel after isothermal treatment is shown in Figure 21. For the specimen held at 650 ºC for 900 s, only a small amount of ferrite is formed, while at 600 ºC and 550 ºC the main product of isothermal transformation is polygonal ferrite and/or quasi-polygonal ferrite. The quantity of these phases obviously decreases with decreasing temperature. Therefore, the nose temperature of reconstructive transformation should be at around 600 ºC. However, while isothermally treated at 500 ºC, most of the austenite transforms into an intermediate transformation microstructure of acicular ferrite and/or bainite.

It can be concluded from all the experimental results presented above that there are two transformation temperature windows for the Mn-Cr-Nb^{+} steel. One is at around 600 ºC, in which polygonal ferrite and quasi-polygonal ferrite are formed. At 550 ºC however, austenite is in a metastable state, the transformation is restrained, so only a small amount of grain boundary allotriomorphic ferrite is formed. Then at around 500 ºC, an intermediate transformation microstructure, such as bainite, can be obtained. Therefore, in order to control the acicular ferrite and bainite microstructure, the steel should be cooled down below 500 ºC.

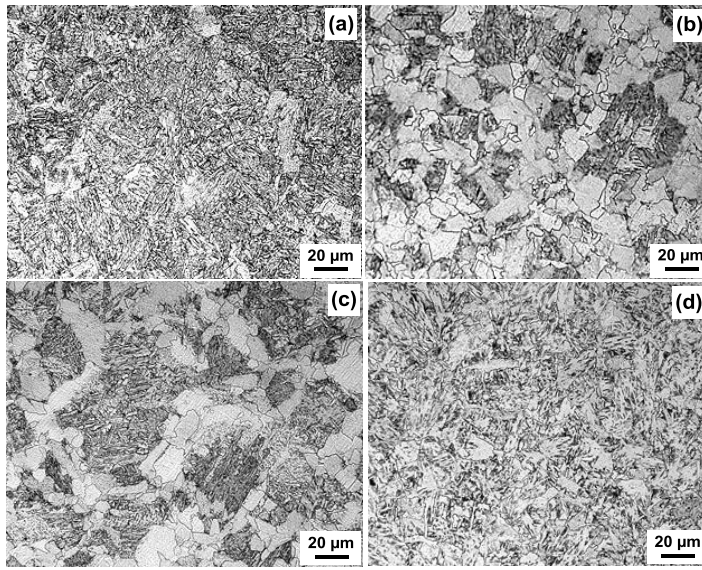

Figure 21. Microstructure of Mn-Cr-Nb^{+} steel after isothermal treatment at different temperatures for 900 s; (a) 650 ºC, (b) 600 ºC, (c) 550 ºC, (d) 500 ºC.

Thermal simulation samples of Φ8 mm × 15 mm were obtained to study the optimum accelerated cooling stop temperature of the Mn-Cr-Nb^{+} steel. The specimens were heated to 1200 ºC at 20 ºC/s, soaked for 300 s, compressed at 850 ºC for 30%, accelerated cooled to 600, 550, 500, 450 ºC, respectively at a rate of 10 ºC/s, and then quenched to room temperature. The influence of different accelerated cooling stop temperatures on phase transformation is shown in Figure 22. It can be seen from Figure 22(a) that the microstructure of the specimen cooled to 600 ºC and then quenched is mainly composed of lath bainite and/or martensite formed during quenching, while after continuous accelerated cooling to 550 ºC, Figure 22(b), only a small amount of acicular ferrite is formed on transformation. After cooling to 500 ºC, Figure 22(c), the microstructure is mostly composed of acicular ferrite. The black spots dispersed in the matrix are the product of quenched residual austenite (MA phase). It can be clearly seen from Figure 22(d) that after cooling to 450 ºC at a rate of 10 ºC/s the transformation to intermediate phase is almost totally completed, and both the amount and size of the MA constituents decrease.

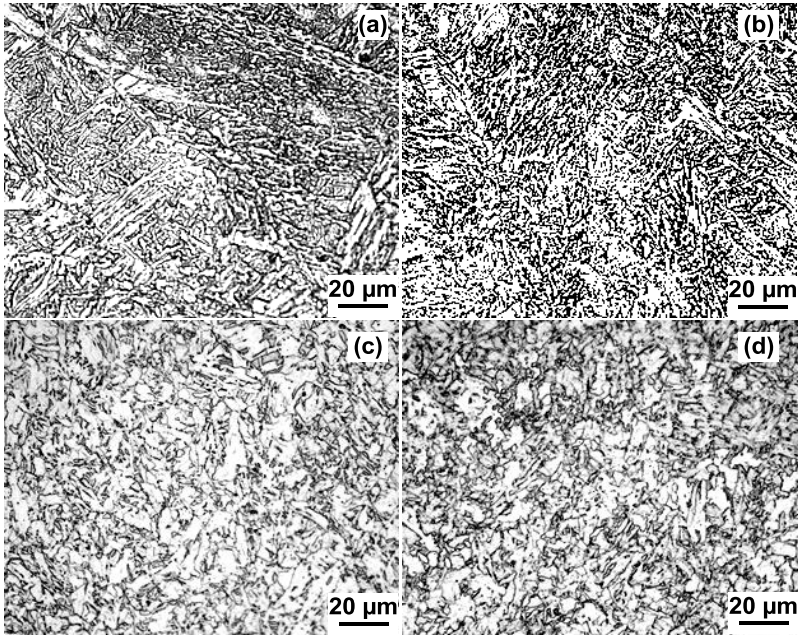

Figure 22. Microstructure after quenching at different temperatures after accelerated cooling at 10 °C /sec; (a) 600 °C, (b) 550 °C, (c) 500 °C, (d) 450 °C.

Conclusions

1. Analysis of stress relaxation data has shown that in the absence of precipitates, the recrystallization behavior of higher Nb steels is time dependent. At decreasing temperatures the recrystallization kinetics require a longer incubation time and longer finish time. This characteristic of higher Nb steel creates a new temperature window around 1000 ºC, without showing obvious accelerated softening by recrystallization as well as no suppressed softening by precipitation. Homogeneous and fine grains are generated prior to the finish rolling in which austenite grains will be fully flattened. This improvement of prior austenite grain condition has a large positive effect on the final properties of the steel.

2. The results of multi-pass rolling simulation indicate that higher Nb can suppress the softening between passes. It may also increase the possibility of partial DRX caused by excessive strain accumulation during hot strip finish rolling. Therefore the start temperature of finish rolling should be lower than 940 °C to fully flatten austenite grains and to accumulate strain or S_v.

3. Analysis of isothermal heat treatment and continuous cooling transformation data and microstructures of Nb and Mo alloyed low carbon steel, makes it clear that in order to obtain an ideal microstructure, the cooling rate after rolling should be controlled to more than 10 ºC/s and the final end cooling temperature should be controlled to below 450 ºC. Addition of Mo can retard the transformation to ferrite and pearlite and produce more acicular ferrite in higher Nb bearing steels at lower cooling rates.

Acknowledgement

This work was supported by the National Basic Research Program of China ("973" Program). The authors are grateful for the support from CITIC and CBMM.

References

1. L.J. Cuddy, *Thermomechanical Processing of Microalloyed Austenite,* ed A.J. DeArdo, G.H. Ratz, and P.J. Wray (Warrendale, PA: The Metallurgical Society of AIME, 1982), 129.

2. K. Hulka, J.M. Gray, and F. Heisterkamp, "Metallurgical Concept and Full-scale Testing of a High Toughness, H2S Resistant 0.03% C-0.10% Nb Steel" (Niobium Technical Report NbTR16/90[R], Companhia Brasileira de Metalurgia & Mineração, Sao Paulo, Brazil, 1990).

3. C.L. Miao et al., "Recrystallization and Strain Accumulation Behaviors of High Nb-bearing Line Pipe Steel in Plate and Strip Rolling," *Materials Science and Engineering A*, 527 (2010), 4985-4992.

4. C.L. Miao et al., "Recrystallization, Precipitation Behaviors and Refinement of Austenite Grains in High Mn High Nb Steel," *Metallurgical and Materials Transactions A*, 43 (2012), 665-676.

5. L.P. Karjalainen, "Stress Relaxation Method for Investigation of Softening Kinetics in Hot Deformation," *Materials Science and Technology*, 11 (6) (1995), 557-565.

6. C.L. Miao et al., "Studies on Softening Kinetics of Niobium Microalloyed Steel Using Stress Relaxation Technique," *Frontiers of Materials Science in China*, 4 (2) (2010), 197-201.

7. J. Kliber and I. Schindler, "Recrystallization/Precipitation Behavior in Microalloyed Steels," *Journal of Materials Processing Technology*, 60 (1996), 597-602.

8. W.J. Liu and J.J. Jonas, "A Stress Relaxation Method for Following Carbonitride Precipitation in Austenite at Hot Working Temperatures," *Metallurgical Transactions A*, 19A (1988), 1430-1413.

9. T.M. Maccagno et al., "Determination of Recrystallization Stop Temperature from Rolling Mill Logs and Comparison with Laboratory Simulation Results," *Iron and Steel Institute of Japan International*, 34 (11) (1994), 917-922.

10. T.X. Cui et al., “Effect of the Composition and Process on Microstructure and Properties of X80 Pipeline Hot Strip Steel,” *Iron and Steel Institute of Japan International*, 44 (2009), 55-59.

11. H.S. Zurob et al., “Analysis of the Effect of Mn on the Recrystallization Kinetics of High Nb Steel: An Example of Physically-based Alloy Design,” *Iron and Steel Institute of Japan International*, 45 (2005), 713-722.

12. A.I. Fernández, P. Uranga, and B. López, “Dynamic Recrystallization Behavior Covering a Wide Austenite Grain Size Range in Nb and Nb–Ti Microalloyed Steels,” *Materials Science and Engineering A*, 361 (2003), 367-376.

13. J.X. Dong, F. Siciliano, and J.J. Jonas, “Effect of Silicon on the Kinetics of Nb(C,N) Precipitation During the Hot Working of Nb-bearing Steels,” *Iron and Steel Institute of Japan International*, 40 (6) (2000) 613-618.

14. K. Minami et al., “Mathematical Modeling of Mean Flow Stress During the Hot Strip Rolling of Nb Steels,” *Iron and Steel Institute of Japan International*, 36 (12) (1996), 1507-1515.

15. C.L. Miao, G.D. Zhang, and C.J. Shang, “Effect of Nb Content on Hot Flow Stress, Dynamic Recrystallization and Strain Accumulation Behaviors in Low Carbon Bainitic Steel,” *Materials Science Forum*, 62 (2010), 654-656.

16. C.L. Miao et al., “Grain Refinement and Microstructure Control of HTP X80 Pipeline Steel,” *Iron and Steel Institute of Japan International*, 3 (015) (2009).